

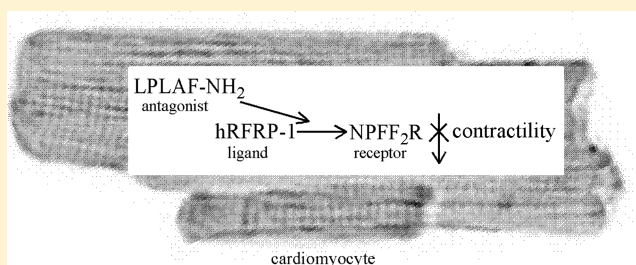
Structure–Activity Studies of RFamide-Related Peptide-1 Identify a Functional Receptor Antagonist and Novel Cardiac Myocyte Signaling Pathway Involved in Contractile Performance

Ruthann Nichols,^{*,†,‡,§,||} Chloe Bass,^{‡,∞} Leslie Demers,^{§,∞} Brian Larsen,^{||,∞} Elton Li,[§] Nathan Blewett,^{||} Kimber Converso-Baran,[⊥] Mark W. Russell,[⊥] and Margaret V. Westfall[#]

[†]Department of Biological Chemistry, [‡]Undergraduate Chemistry Honors Research Program, [§]Undergraduate Biochemistry Honors Research Program, ^{||}Graduate Program in Biomedical Sciences, [⊥]Department of Pediatrics and Communicable Diseases, and [#]Department of Cardiac Surgery, The University of Michigan Medical School, Ann Arbor, Michigan 48109, United States

S Supporting Information

ABSTRACT: Human RFamide-related peptide-1 (hRFRP-1, MPHSFANLPLRF-NH₂) binds to neuropeptide FF receptor 2 (NPFF₂R) to dramatically diminish cardiovascular performance. hRFRP-1 and its signaling pathway may provide targets to address cardiac dysfunction. Here, structure–activity relationship, transcript, Ca²⁺ transient, and phospholabeling data indicate the presence of a hRFRP-1 pathway in cardiomyocytes. Alanyl-substituted and N-terminal truncated analogues identified that R¹¹ was essential for activity, hRFRP-1_(8–12) mimicked hRFRP-1, and [A¹¹]hRFRP-1_(8–12) antagonized the effect of hRFRP-1 in cellular and integrated cardiac performance. RFRP and NPFF₂R transcripts were amplified from cardiomyocytes and heart. Maintenance of the Ca²⁺ transient when hRFRP-1 impaired myocyte shortening indicated the myofilament was its primary downstream target. Enhanced myofilament protein phosphorylation detected after hRFRP-1 treatment but absent in [A¹¹]hRFRP-1_(8–12)-treated cells was consistent with this result. Protein kinase C (PKC) but not PKA inhibitor diminished the influence of hRFRP-1 on the Ca²⁺ transient. Molecules targeting this pathway may help address cardiovascular disease.



■ INTRODUCTION

Peptides act to regulate cardiovascular function, yet the peptidergic contribution to cardiac dysfunction is not completely understood. Identifying and characterizing a small cardioregulatory peptide is an attractive approach to drug discovery because of its size and ability to serve as a high-affinity ligand. In addition, the mechanisms involved in the synthesis and signaling of physiologically active peptides may be a rich source of target molecules for drug discovery. The design of an antagonist to peptidergic ligand binding at a G-protein-coupled receptor (GPCR) is a promising avenue to discover progenitor molecules for drug development and therapeutic strategies to address cardiac dysfunction.

Physiologically active peptides can often be grouped together based on a common motif, and frequently, functionally similar orthologous structures exist in vertebrates and invertebrates. Members of one cardioregulatory peptide family are related by an identical RF-NH₂ C terminus. The first RF-NH₂-containing peptide identified was the cardioactive tetrapeptide FMRF-NH₂.¹ Subsequently, numerous cardioregulatory FMRF-NH₂-related peptides (FaRPs) were identified including RFamide-related peptide-1 (RFRP-1) in mammals.^{2,3} The FaRP family can be further divided into groups based on XRF-NH₂, where X defines the subfamily.

Human RFRP-1 (hRFRP-1) is encoded in a polypeptide precursor that undergoes post-translational modification to produce the naturally occurring peptide MPHSFANLPLRF-NH₂.⁴ A structurally similar RFRP-1 peptide was isolated from bovine hypothalamus⁵ and predicted from the rat RFRP gene.^{2,3} Vertebrate RFRP-1 peptides and the invertebrate myosuppressins,⁶ which also dramatically decrease cardiac contractility, are members of the LRF-NH₂ FaRP subfamily. The mammalian peptide is of interest in cardiovascular research because RFRP-1 immunoreactive material is expressed in regions of the central nervous system involved in cardiac regulation.^{5,7,8} In addition, hRFRP-1 was recently shown to dramatically diminish cellular and integrated cardiac performance.⁹ Another RF-NH₂-containing peptide, hRFRP-3 (VPNLPQRF-NH₂), may also be processed from the same precursor; it is not a member of the LRF-NH₂ subfamily.

Two GPCR proteins designated NPFF receptor 1 (NPFF₁R) and NPFF receptor 2 (NPFF₂R), which bind RFRP peptides, are expressed in brain tissue.^{3–5,7,8,10,11} Although RFRP-1 dramatically decreases cardiac performance dose dependently, there is no published report describing its structure–activity

Received: May 31, 2012

Published: August 21, 2012

relationship (SAR) or a functional antagonist or signaling pathway for its effect on cardiac performance. Delineating SAR is a basis to design functional antagonists to a GPCR for drug discovery. In this study, the method used to establish activity was previously described, that is, the effect of the peptide on cardiac contractility as measured in isolated myocytes.⁹ Those analogues identified as inactive may still bind but not activate the peptidergic signaling pathway. Thus, testing RFRP-1 activity in the presence of inactive analogues may provide information useful in the design of a receptor antagonist. Also, SAR data may identify an active core, the shortest length of amino acids with an effect equivalent in magnitude to or that mimics hRFRP-1 activity. Small, highly specific molecules are preferred candidates for drug discovery in part because of delivery, synthesis, and costs. In addition, components of transduction mechanisms are targets for the development of therapeutic strategies to treat disease states such as heart failure.

An aim of this study was to test the hypothesis that the active core of hRFRP-1 influencing cardiac performance is present in its C terminus. This prediction was based on the presence of a strictly conserved LRF-NH₂ in cardioinhibitory FaRPs. Also, C-terminal amidation is well established to prevent inactivation by peptidases¹² and thus is often required for bioactive peptide activity. To test this hypothesis, the SAR for the effect of hRFRP-1 on cardiac performance was investigated to identify residues critical to activity and the shortest length of amino acids that mimicked the effect of the parent peptide. A second aim was to test the hypothesis that an inactive analogue may bind but not activate the RFRP-1 receptor signaling pathway. To test this hypothesis, the effect of hRFRP-1 on contractility was measured in the presence of individual analogues that were inactive. An additional aim was to test the hypothesis that molecular components of a hRFRP-1 signaling pathway exist in cardiac myocytes. This prediction was based on the observation that physiological concentrations of hRFRP-1 act directly on isolated cardiomyocytes to dramatically diminish cardiac contractility.⁹ To test this hypothesis, the presence of RFRP and NPFRR transcripts was investigated in isolated rat cardiac myocytes and heart and human heart. Another aim was to investigate the hypothesis that calcium influx and phosphorylation of downstream targets are involved in the cellular response to hRFRP-1 applied to cardiomyocytes. This prediction was based on the established roles of calcium and kinases in cardiac contractility. In addition, a protein kinase C (PKC) inhibitor blocks hRFRP-1 activity in isolated cardiomyocytes.⁹

The hRFRP-1 SAR provides powerful information to guide research on the discovery of progenitor molecules for drug development. Knowledge of components of the hRFRP-1 cardiac signaling pathway aids in identifying molecular targets to develop strategies to prevent or attenuate cardiovascular dysfunction.

RESULTS

Structure–Activity Relationship. In an earlier study, hRFRP-1, MPHSFANLPLRF-NH₂, was shown to dramatically decrease cardiac performance in a dose dependent manner; best-fit EC₅₀ values were 5×10^{-10} , 5×10^{-11} , and 5×10^{-11} M for peak shortening amplitude and shortening and relengthening rates of myocytes, respectively.⁹ The dose response effect demonstrated a robust response for 10 nM hRFRP-1; thus, this concentration was chosen to test the peptides and analogues used in this study.

One goal of the current study was to delineate the SAR for the effect of this peptide, which in turn provided data to design receptor agonists and antagonists for functional and mechanistic studies. Two sets of analogues, alanyl-substituted and N-terminal truncations, were chosen to provide independent but complementary data to identify the amino acids and peptide length required for activity. Each analogue was analyzed at 10 nM. The peak shortening amplitude and shortening (departure velocity) and relengthening (return velocity) rates were measured in myocytes over 20 min. Controls included the analysis of 10 nM unsubstituted parent peptide and the media vehicle only, without peptide or analogue. In addition, each inactive analogue was evaluated to assess its ability to limit the activity of the parent peptide to gain insight into the design of a functional antagonist to block the influence of hRFRP-1 on cellular and integrated cardiac performance.

Alanyl-Substituted hRFRP-1 Analogues. Alanyl-substituted analogues were used to delineate the SAR by systematically replacing each residue, one by one, with alanine to investigate the contribution of the amino acid side chain to hRFRP-1 activity in isolated cardiac myocytes. On the basis of physical characteristics of the side chains, a naturally occurring alanine at position 6 (A⁶) was replaced with glycine. The analogue nomenclature used followed established convention and is detailed in the Experimental Section.

On the basis of the alanine scan data, the replacement of only one residue in hRFRP-1, R¹¹, produced an inactive analogue with no effect on peak shortening amplitude or shortening and relengthening rates compared to the unsubstituted parent peptide (Figure 1, Table 1). Application of media alone or the [A¹¹]hRFRP-1 analogue produced no substantial change in the peak shortening amplitude or shortening and relengthening rates and was significantly different from the effect of 10 nM hRFRP-1 (Figure 1, Table 1). Substitution with alanine or glycine for other amino acids did not change activity compared to hRFRP-1, the unsubstituted parent peptide, for all three parameters measured. However, some substitutions generated analogues with different magnitude influences on function. For example, [A⁷]hRFRP-1 and [A⁹]hRFRP-1 had slightly less impact than the unsubstituted parent peptide (Figure 1, Table 1). Yet substitution in the N-terminal portion of the peptide to produce [A³]hRFRP-1 resulted in an analogue that was more effective in its ability to decrease cardiac myocyte performance compared to the parent peptide. [A³]hRFRP-1, MPAS-FANLPLRF-NH₂, decreased the shortening rate by 23% more than the parent hRFRP-1 peptide (Table 1).

Overall, the results of the hRFRP-1 alanine scan indicated that a conserved residue in the C-terminal hexamer was critical for modulation of cardiac myocyte function and that at least one residue in the N-terminal extension modified activity. The finding that amino acids in the C-terminal portion of the peptide were important for activity was consistent with the strict conservation of the residues in RFRP-1 sequences from several species (see Supporting Information for RFRP-1 sequence alignment).

N-Terminal Truncation hRFRP-1 Analogues. Our second approach for evaluating the hRFRP-1 SAR was to examine the importance of peptide length in modulating contractile function. These studies were carried out by systematically removing a residue, one at a time, to generate a series of N-terminal truncated analogues. The analogue nomenclature used followed established convention and is detailed in the Experimental Section. Analysis of truncations

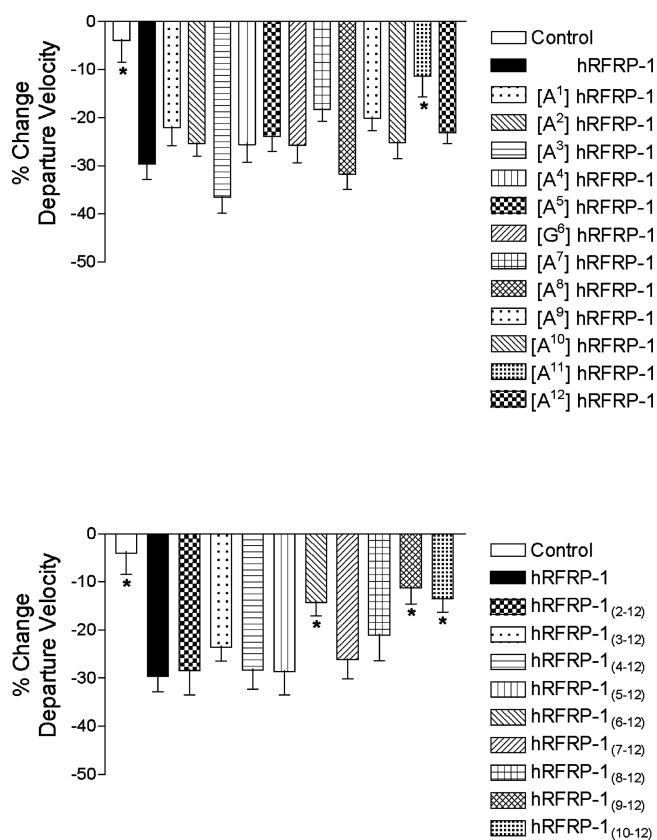


Figure 1. Alanyl-substituted and N-terminal truncated hRFRP-1 analogues affect sarcomere length shortening rate (departure velocity) in cardiac myocytes. The effects of 10 nM analogues are reported as percent (%) change relative to baseline \pm SEM (error bars). An asterisk (*) indicates significance ($p \leq 0.05$) relative to hRFRP-1. Control is media only.

generated by removing an amino acid at the N terminus was the strategy taken because an amidated C terminus is often required in bioactive peptides.¹² Additionally, the high degree of structure identity in the C terminus of FaRPs is indicative of it playing an important role in activity and/or binding. The RFRP-1 consensus structure is X¹PX²SX³ANLPLRF-NH₂ with minimal variability in positions X¹, X², and X³ (see Supporting Information for RFRP-1 sequence alignment).

Truncation of the first four amino acids to generate hRFRP-1₍₂₋₁₂₎, hRFRP-1₍₃₋₁₂₎, hRFRP-1₍₄₋₁₂₎, and hRFRP-1₍₅₋₁₂₎ did not significantly alter the ability of the analogues to decrease peak shortening amplitude or shortening and relengthening rates compared to the full-length parent peptide (Figure 1, Table 1). These results are consistent with the conclusion that the first four residues in the N-terminal sequence did not play a critical role in all three parameters measured. An alternative explanation is that the amino acids that remained in the truncated analogues were capable of maintaining a distinct conformation(s) that was active and mimicked the influence of hRFRP-1 on cardiac contractility.

Removal of F⁵ generated ANLPLRF-NH₂, an analogue that did not substantially attenuate contractile function compared to hRFRP-1 (Figure 1, Table 1). Interestingly, the removal of the flexible A⁶ residue that produced NLPLRF-NH₂ restored activity, indicating that the analogue took on an active conformation. Analysis of additional truncations identified the active core, LPLRF-NH₂ (Figure 1, Table 1). Further

truncations produced hRFRP-1₍₉₋₁₂₎ and hRFRP-1₍₁₀₋₁₂₎, which were inactive (Figure 1, Table 1). No additional truncated analogues were analyzed because the remaining amino acids and post-translational modification, RF-NH₂, were not unique to hRFRP-1 but common to all FaRPs and thus would not contain the ligand–receptor specificity needed for drug design.

Functional Antagonist. A second goal of this study was to develop a functional antagonist of the effect of hRFRP-1 on cardiac contractility. Although inactive alanyl-substituted and N-terminal truncated analogues provided information necessary to design a receptor antagonist, these analogues themselves were not attractive candidates. The inactive C-terminal amidated dodecamer [A¹¹]hRFRP-1 was a relatively large precursor to serve as a first generation antagonist; a shorter sequence is considered more desirable because it may be easier to deliver physiologically and to decrease the complexity, cost, and time of synthesis. The presence of the active analogues hRFRP-1₍₇₋₁₂₎ and hRFRP-1₍₈₋₁₂₎ within the structure of the inactive analogue hRFRP-1₍₆₋₁₂₎ did not make ANLPLRF-NH₂ an ideal candidate. Also, the inactive truncated analogues hRFRP-1₍₉₋₁₂₎ and hRFRP-1₍₁₀₋₁₂₎ would not be high affinity ligands because of limited peptide length and would not be specific to hRFRP-1 because of sequence conservation within the FaRP family. Instead, data from the two SAR approaches led to LPLAF-NH₂; its design was based on the truncated amidated pentamer remaining active and being hRFRP-1 specific and the substitution of R¹¹ with A which resulted in an inactive analogue. Thus, [A¹¹]hRFRP-1₍₈₋₁₂₎ was a small molecule with the potential to act as an antagonist to block the effect of hRFRP-1 on cardiac contractility.

In order to investigate the potential for LPLAF-NH₂ to act as a RFRP-1 receptor antagonist, the analogue was first tested at 10 nM in isolated rat ventricular cardiac myocytes and found to lack the ability to modulate contractility relative to the parent peptide (Figure 2). Next, LPLAF-NH₂ and hRFRP-1 were applied in equal concentrations (10 nM) to isolated cardiac myocytes. In these studies, LPLAF-NH₂ acted as an antagonist to the hRFRP-1 receptor by limiting parent peptide induced decreases in cardiac myocyte contractile performance (Figure 2). Although 10 nM hRFRP-1 decreased peak shortening amplitude by $27 \pm 3\%$ and slowed the rates of shortening and relengthening by $30 \pm 3\%$ and $32 \pm 3\%$, respectively, addition of 10 nM LPLAF-NH₂ with 10 nM hRFRP-1 attenuated this response by approximately 50% (Figure 2).

Further analysis of the ability of LPLAF-NH₂ to serve as an antagonist was investigated in vivo using tail vein injection to deliver the analogue to mouse myocardium. The functional impact of this analogue was monitored by serial echocardiography and compared to equal amounts of analogue and parent peptide delivered together and to an equal volume of physiological saline that served as a control. As expected, [A¹¹]hRFRP-1₍₈₋₁₂₎ itself was inactive in this in vivo animal model. Delivery of LPLAF-NH₂ together with the parent peptide attenuated the ability of hRFRP-1 to diminish function measured by decreases in ejection fraction (EF) and fractional shortening (FS, Table 2). Thus, [A¹¹]hRFRP-1 proved to act as a functional antagonist of the cardiac actions of hRFRP-1 under cellular and integrated conditions.

In literature, the RF-NH₂ derivative RF9¹³ is reported to demonstrate antagonist activity at NPPF receptors. Recently, RF9 was shown to antagonize the effect of RFRP-1 to limit vertebrate food intake activity;¹⁴ however, to our knowledge,

Table 1. Influence of 10 nM hRFRP-1, Analogues, and Saline Reported as % hRFRP-1 Activity for Peak Shortening Amplitude (peak s) and Rates of Shortening (Departure Velocity, dep v) and Relengthening (Return Velocity, ret v)^a

		% hRFRP-1 activity					
		peak s	<i>p</i>	dep v	<i>p</i>	ret v	<i>p</i>
hRFRP-1	MPHSFANLPLRF-NH ₂	100 ± 14		100 ± 15		100 ± 12	
[A ¹]hRFRP-1	APHSFANLPLRF-NH ₂	50 ± 9	**	74 ± 15	0.2	55 ± 9	**
[A ²]hRFRP-1	MAHSFANLPLRF-NH ₂	91 ± 14	0.6	85 ± 13	0.5	72 ± 11	0.1
[A ³]hRFRP-1	MPASFANLPLRF-NH ₂	93 ± 20	0.8	123 ± 17	0.3	89 ± 15	0.6
[A ⁴]hRFRP-1	MPHAFANLPLRF-NH ₂	83 ± 12	0.4	86 ± 16	0.6	91 ± 14	0.6
[A ⁵]hRFRP-1	MPHSAANLPLRF-NH ₂	50 ± 16	*	80 ± 14	0.4	51 ± 11	**
[G ⁶]hRFRP-1	MPHSFGNLPLRF-NH ₂	84 ± 16	0.5	86 ± 15	0.6	81 ± 14	0.4
[A ⁷]hRFRP-1	MPHSFAALPLRF-NH ₂	61 ± 12	0.06	61 ± 11	0.07	67 ± 10	0.06
[A ⁸]hRFRP-1	MPHSFANAPLRF-NH ₂	107 ± 16	0.8	107 ± 16	0.8	80 ± 14	0.4
[A ⁹]hRFRP-1	MPHSFANLALRF-NH ₂	55 ± 9	*	67 ± 12	0.2	54 ± 8	**
[A ¹⁰]hRFRP-1	MPHSFANLPAF-NH ₂	76 ± 15	0.3	85 ± 14	0.5	56 ± 11	**
[A ¹¹]hRFRP-1	MPHSFANLPLAF-NH ₂	19 ± 18	*	38 ± 15	*	15 ± 16	***
[A ¹²]hRFRP-1	MPHSFANLPLRA-NH ₂	89 ± 17	0.6	77 ± 11	0.3	89 ± 16	0.6
hRFRP-1 ₍₂₋₁₂₎	PHSFANLPLRF-NH ₂	118 ± 19	0.4	96 ± 22	0.9	78 ± 10	0.2
hRFRP-1 ₍₃₋₁₂₎	HSFANLPLRF-NH ₂	49 ± 8	**	79 ± 15	0.4	65 ± 10	0.06
hRFRP-1 ₍₄₋₁₂₎	SFANLPLRF-NH ₂	63 ± 14	0.08	96 ± 19	0.9	78 ± 12	0.2
hRFRP-1 ₍₅₋₁₂₎	FANLPLRF-NH ₂	86 ± 24	0.6	97 ± 22	0.9	88 ± 15	0.5
hRFRP-1 ₍₆₋₁₂₎	ANLPLRF-NH ₂	54 ± 13	*	48 ± 12	*	60 ± 13	*
hRFRP-1 ₍₇₋₁₂₎	NLPLRF-NH ₂	63 ± 11	0.06	89 ± 18	0.6	72 ± 13	0.1
hRFRP-1 ₍₈₋₁₂₎	LPLRF-NH ₂	87 ± 22	0.6	71 ± 22	0.3	82 ± 14	0.4
hRFRP-1 ₍₉₋₁₂₎	PLRF-NH ₂	48 ± 8	**	38 ± 13	**	36 ± 9	***
hRFRP-1 ₍₁₀₋₁₂₎	LRF-NH ₂	59 ± 15	0.08	45 ± 12	*	49 ± 15	*
hRFRP-3	VPNLPQRF-NH ₂	5 ± 10	**	-15 ± 13	**	-6 ± 17	***
control	saline	39 ± 13	**	13 ± 16	***	27 ± 15	***

^aAsterisks were used to represent *p* values (*, *p* ≤ 0.05; **, *p* ≤ 0.01; ***, *p* ≤ 0.001).

the RF-NH₂ derivative remains untested in cardiovascular physiology. To determine its functional capacity to antagonize the effect of hRFRP-1 on cardiac contractility, we first applied 10 nM RF9 alone on isolated rat cardiac myocytes and found it did not influence performance (Figure 3). Its effect was significantly different from 10 nM hRFRP-1 applied alone and similar to a control, applying media alone. The effect of 10 nM hRFRP-1 in the presence of 10 nM RF9 was not significantly different from peptide alone (Figure 3). These results indicated that RF9 did not block peptidergic activity, and thus, the RF-NH₂ derivative was not a functional antagonist of the hRFRP-1 effect on contractile performance in cardiac myocytes.

RFRP-1 Cardiac Myocyte Signaling Pathway. Delineating the pathway necessary for hRFRP-1 signaling in the myocardium may be useful for future drug development. The ability of nanomolar amounts of hRFRP-1 to dramatically decrease myocyte contractility suggests this peptide is likely a physiological signaling mechanism employed to modulate contractile function in the intact myocardium. Furthermore, hRFRP-1 acts in a dose-dependent manner on ventricular cardiac myocytes.⁹ The well-defined SAR described in this study also is consistent with downstream activation of one or more signal transduction pathways by RFRP-1 in cardiac myocytes, although there are no previous reports describing this pathway(s) in myocardium. To this end, we explored the presence of the peptide and its receptor protein in isolated cardiac myocytes and heart.

Polymerase chain reaction (PCR) amplification established hRFRP-1 signaling components were present in isolated rat ventricular cardiac myocytes and heart and human heart through amplification of transcripts which were sequenced (see Supporting Information for primer sequences, predicted

melting temperatures, and amplified product sizes). The sequence data from rat cardiac myocytes and heart and human heart mRNA showed that RFRP and NPFF₂R transcripts were present (Table 3). Although the experiment was conducted, the NPFF₁R transcript was not amplified from rat cardiac myocytes. However, NPFF₁R transcript was amplified from rat brain mRNA. Negative controls for this group of experiments included 26RFamide (26RFa), a brain FaRP that lacks influence on contractile performance in isolated myocytes⁹ and its receptor, GPR103.^{15,16} Amplification of rat cardiomyocyte mRNA did not identify 26RFa or GPR103 transcripts (Table 3). The cardioregulatory peptide ET-1¹⁷ served as a positive control and, as expected, was amplified from rat cardiac myocytes and heart and human heart mRNA (Table 3). All products are known to be present in the central nervous system, and as expected, each transcript was detected in rat brain (Table 3). The sequences of amplified products were exact matches for the data deposited at the NCBI (see Supporting Information for PCR product sequences). Additional controls included no mRNA template, no reverse transcriptase, and no primers, and in each case no product was amplified.

Further insight into this cardiac signaling pathway was gained by measuring RFRP and NPFF₂R expression using quantitative PCR (qPCR). Unlike the PCR experiments, qPCR provided transcript levels in real time, not sequence data; thus, these two techniques did not produce redundant results. Ribosomal protein L32 (Rpl32) was chosen as the reference transcript because of its stable expression levels in rat ventricular cardiac myocytes, heart, and brain.¹⁸ Brain was chosen as the reference tissue because RFRP, NPFF₂R, and 26RFa transcripts were consistently amplified from rat brain by PCR. (Primer

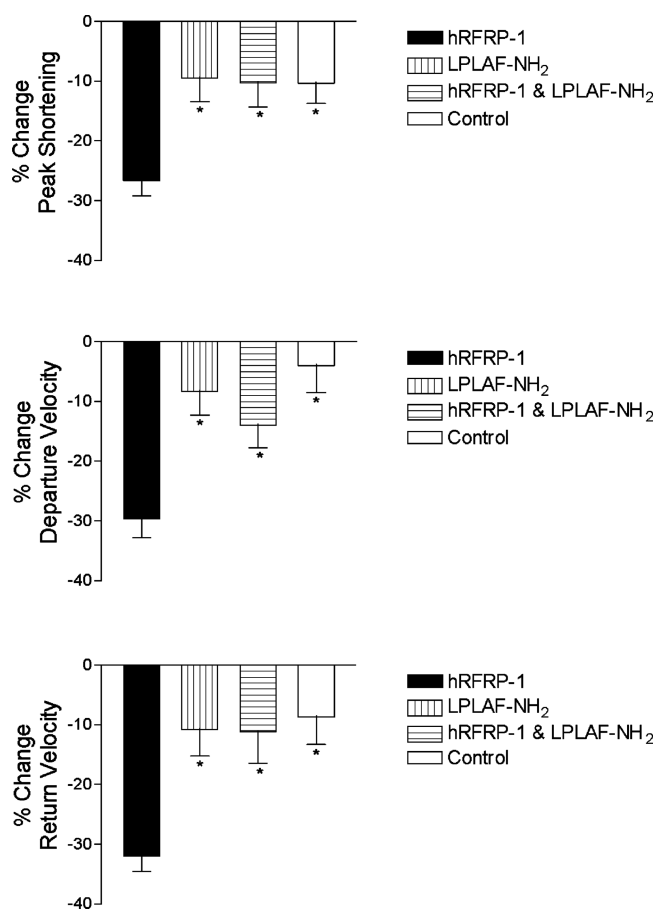


Figure 2. LPLAF-NH₂ investigated as a functional receptor antagonist to hRFRP-1 activity in cardiac myocytes. The effects of 10 nM hRFRP-1, LPLAF-NH₂, hRFRP-1 and LPLAF-NH₂, and control are reported as % change \pm SEM (error bars) for peak shortening amplitude (peak shortening) and the rates of shortening (departure velocity) and relengthening (return velocity) in cardiac myocytes. An asterisk (*) indicates significance ($p \leq 0.05$) relative to hRFRP-1. Control is media only.

Table 2. Mouse Cardiovascular Function Measured in Response to hRFRP-1, LPLAF-NH₂, hRFRP-1 and LPLAF-NH₂ (Each Delivered at 250 nmol/kg bw), and Saline (Control)^a

	% EF	% FS
hRFRP-1	-16 ± 3	-12 ± 2
LPLAF-NH ₂	4 ± 2	4 ± 2
hRFRP-1 + LPLAF-NH ₂	4 ± 2	4 ± 2
saline	7 ± 2	7 ± 2

^aThe average value and standard deviation are reported.

sequences and predicted melting temperatures and qPCR amplified product sizes are in Supporting Information.) The relative expression differences calculated using the comparative threshold cycle (C_T) method^{19,20} demonstrated that the RFRP transcript was expressed in rat cardiac myocytes and heart at $30 \pm 1\%$ and $32 \pm 5\%$ of the level expressed in brain, respectively (Figure 4). Although the 26RfA transcript was not detected in rat ventricular cardiac myocytes, it was detected in whole heart and brain (Figure 4). Similar levels of NPFF₂R transcript were expressed in heart and brain; the NPFF₂R transcript level in cardiac myocytes was $90 \pm 10\%$ of the brain level (Figure 4). A

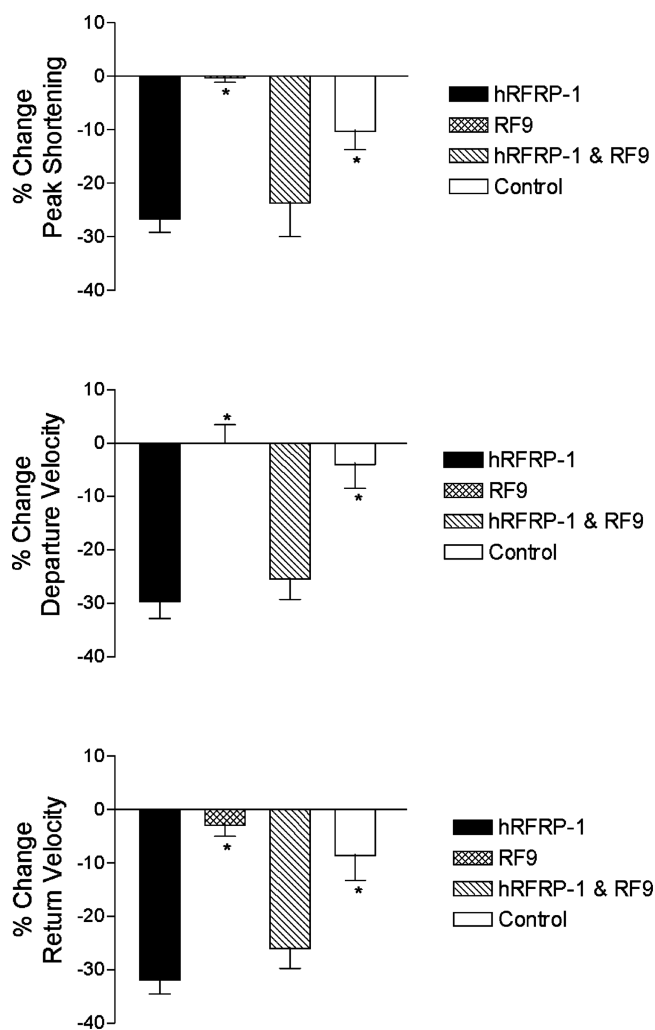


Figure 3. RF9 investigated as a functional receptor antagonist to hRFRP-1 activity in cardiac myocytes. The effects of 10 nM hRFRP-1, RF9, hRFRP-1 and RF9, and control are reported as % change \pm SEM (error bars) for peak shortening amplitude (peak shortening) and the rates of shortening (departure velocity) and relengthening (return velocity) in cardiac myocytes. An asterisk (*) indicates significance ($p \leq 0.05$) relative to hRFRP-1. Control is media only.

Table 3. Peptide and Receptor Transcripts Amplified (+) or Not Amplified (-) from Rat Cardiac Myocyte and Brain mRNA and Human Heart mRNA

	rat cardiac myocyte	rat brain	human heart
RFRP	+	+	+
NPFF ₂ R	+	+	+
26RfA	-	+	+
GPR103	-	+	+
ET-1	+	+	+

similar set of controls described for the PCR studies were used for qPCR controls.

Together, the PCR and qPCR results indicate that the presence and identity of RFRP-1 signaling components in isolated rat ventricular cardiac myocytes, heart, and brain and in human heart are in agreement with the dose response effect of the peptide on cardiac performance. This molecular work is also consistent with the well-defined functional responses reported for the hRFRP-1 SAR in isolated cardiac myocytes.

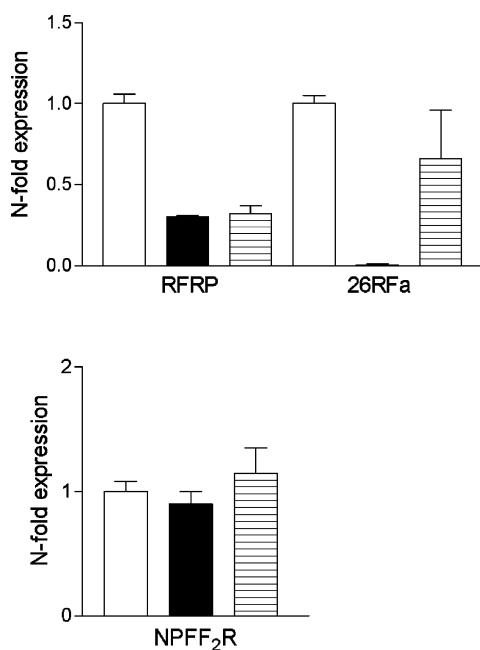


Figure 4. qPCR analysis of peptide and receptor transcript expression in rat brain, cardiac myocytes, and heart. The *N*-fold expression (*y*-axis) levels of RFRP, 26RFa, and NPFF₂R (*x*-axis) in rat brain (open), cardiac myocytes (closed), and heart (horizontal lines) are shown.

The molecular results observed with the 26RFa negative control and its receptor are consistent with the inability of this peptide to influence cardiac myocyte contractile function previously reported.⁹

In addition, hRFRP-3 (VPNLQRF-NH₂) was tested for its ability to influence cardiac contractility in isolated cardiac myocytes (Table 1). Whether hRFRP-3 influenced cardiac performance was evaluated in the same way as all other peptides and analogues in this study. When applied to isolated cardiac myocytes, 10 nM hRFRP-3 was significantly different from the effects of hRFRP-1 on contractile performance; it was similar to the application of saline (Table 1). These data support the conclusion that hRFRP-3 does not activate the cardiomyocyte signaling pathway through which hRFRP-1 influences isolated cardiac myocyte contractility, even though it is also encoded in the RFRP transcript found in heart. These results and SAR data support that the signaling pathway is specific to hRFRP-1 and not a property of other FaRP family members. Thus, the current study provides strong evidence that a RFRP-1-specific pathway is present in the myocardium and that it modulates contractile function.

Ca²⁺ Transient and Signaling. The contribution of the Ca²⁺ transient and potential downstream signaling pathway(s) activated in response to hRFRP-1 were investigated to gain mechanistic insight into the function of this peptide in the heart. First, studies in Fura-2AM loaded rat myocytes determined whether decreases in the cellular Ca²⁺ transient were responsible for diminished myocyte function in response to hRFRP-1. Resting length and basal Ca²⁺ remained comparable before and after 10 nM hRFRP-1 was applied (Figure 5A). Interestingly, the diminished amplitude of peak shortening was associated with an unexpected trend toward an increase, rather than decrease, in the peak cellular Ca²⁺ transient (Figure 5A). This cellular Ca²⁺ transient response to hRFRP-1 was not significantly different from control values; it was clear the diminished peak shortening was not accompanied

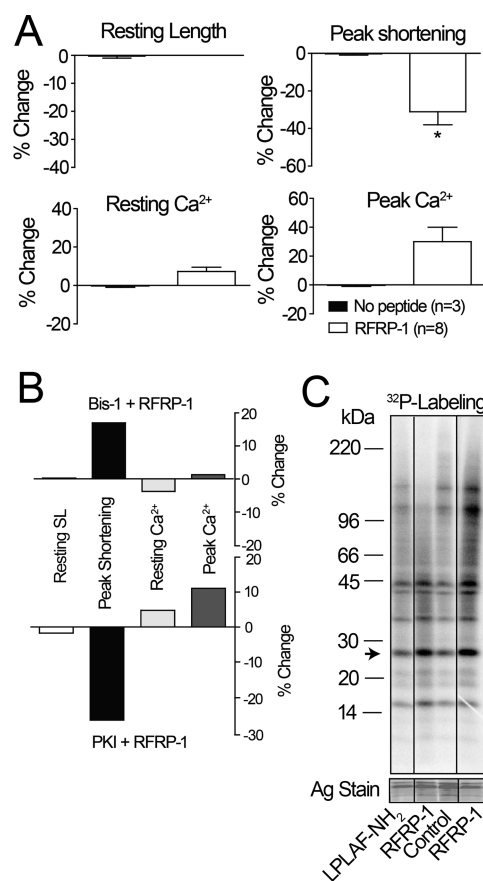


Figure 5. Ca²⁺ transients and myofilament protein phosphorylation were analyzed in response to hRFRP-1. (A) Basal and peak Ca²⁺ transients and peak shortening amplitude in saline versus 10 nM hRFRP-1-treated myocytes. An asterisk (*) indicates significance ($p \leq 0.05$) relative to control (saline). (B) Change in resting length, peak shortening amplitude, resting Ca²⁺, and peak Ca²⁺ in myocytes treated with the PKA inhibitor, PKI, or the PKC inhibitor, Bis-1. Data shown are measurements from $n = 2$ which were representative of results in additional cells. (C) Phosphorylation detected in myocytes (cTnI, arrow) labeled with ³²P-orthophosphate treated with 10 nM LPLAF-NH₂, RFRP-1, or control. Incubation was in the presence of the phosphatase inhibitor, calyculin A (10 nM).

by a similar reduction in peak Ca²⁺ transient. Thus, myofilament proteins rather than Ca²⁺ cycling proteins appeared likely to be the targets for downstream signaling activated by hRFRP-1.

Studies were then conducted to determine if the Ca²⁺ transient response to hRFRP-1 could be blocked with inhibitors of protein kinase C (PKC) and/or PKA pathways. The two kinase pathways are known upstream modulators of contractile function that produce divergent functional effects on the myofilament.^{21,22} Specifically, PKA activation enhances contraction and relaxation, although PKC more often is associated with diminished myofilament function. The response to hRFRP-1 in the presence of the PKA inhibitor PKI was comparable to its original response with diminished peak shortening amplitude and a trend toward elevated Ca²⁺ transients (Figure 5B). In contrast, the diminished peak shortening amplitude and the trend toward enhanced Ca²⁺ transients in response to hRFRP-1 were attenuated by the PKC inhibitor bis-indolylmaleimide, Bis-1 (Figure 5B).

The ability of hRFRP-1 to produce significant changes in myofilament protein phosphorylation was then analyzed in radiolabeled myocytes. In these studies, a band migrating at the molecular weight (between 20 and 30 kDa markers) associated with cardiac troponin I (cTnI) was phosphorylated in response to 10 min of treatment with 10 nM hRFRP-1 compared to controls (no peptide) or myocytes treated with a similar dose of LPLAF-NH₂ (Figure 5C, arrow). Phosphorylation of cTnI is involved in relaxation in cardiac myocytes.²³ There were no consistent increases in the phosphorylation of proteins in the control experiments. Although phosphorylation of cTnI is unlikely to explain the overall reduction in contractile function, this result indicated that downstream myofilament proteins are targets for signaling cascade(s) activated by hRFRP-1.

DISCUSSION

Our results strongly support the conclusion that a unique RFRP-1-specific signaling pathway exists in mammalian ventricular cardiac myocytes. Detailed SAR analysis laid the foundation for the design of a functional receptor antagonist to a novel hRFRP-1-specific cardiac signaling pathway. Cellular and animal studies showed that a first generation NPFF₂R antagonist, LPLAF-NH₂, inhibited the ability of hRFRP-1 to diminish both cellular and integrated cardiac performance. Additionally, gene expression experiments provided evidence that RFRP-1 and NPFF₂R are present in myocytes and heart, which play important roles in regulating cardiac contractility. Our studies also provided additional support that PKC signaling is activated by hRFRP-1. Finally, we determined that myofilaments are targets for downstream phosphorylation in response to hRFRP-1. Collectively, these data are consistent with RFRP-1 acting as a novel peptide involved in modulating *in vivo* cardiac contractile function. Heart disease is a leading cause of death in the United States.²⁴ Identification of hRFRP-1 as a negative modulator of contractile function may provide an opportunity to develop therapeutic strategies targeting its transduction pathway in patients with heart failure.

Prior to this study, there were no published RFRP-1 SAR data or functional NPFF₂R antagonist described in cardiovascular physiology. The SAR data confirmed that the active core was present in the C terminus; additional observations were also made. The lesser magnitude influences of [A⁷]hRFRP-1 and [A⁹]hRFRP-1 reinforced the importance of the C-terminal hexamer and suggested that hRFRP-1 contains a conformation(s) required for activity that may be perturbed by substitution of a specific amino acid but can be stabilized by the presence of the remaining naturally occurring residues. However, an alternative explanation cannot be ruled out; that is, an analogue may take on a distinct, yet active conformation that is different in effectiveness.

Our detailed studies on the full-length peptide resulted in several novel findings; frequently, the focus of SAR RF-NH₂ analysis is directed toward the C terminus because of its high degree of structure conservation among species.²⁵ The alanine scan revealed the enhanced ability of [A³]hRFRP-1 to decrease cardiac myocyte performance (Figure 1, Table 1). Its 23% greater reduction in shortening rate compared to hRFRP-1 may result from a more flexible conformation that occurs when H³ is replaced in the alanyl-substituted analogue. Considerable differences in length, aromaticity, and hydrophilicity between histidine and alanine side chains are expected to contribute to an overall increase in conformational flexibility. This result suggests that the potency of the parent peptide may be

increased through the design of analogues to the N-terminal extension.

N-Terminal truncated analogues analysis demonstrated that removal of F⁵ resulted in ANLPLRF-NH₂, an analogue with significantly attenuated ability to modify contractile function (Figure 1, Table 1). Loss of the bulky, aromatic side chain in F⁵ may have diminished peptide function because it is directly involved in ligand–receptor interaction. The remaining small, hydrophobic side chain in the adjacent A⁶ may be unable to compensate for the loss of F⁵. However, this result is in contrast to the outcome observed with the alanyl-substituted analogue data, where the F⁵A substitution did not significantly reduce activity. Thus, a more likely explanation may be that the N-terminal A⁶ in hRFRP-1_(6–12) increased flexibility in the peptide and disrupted the conformation required for activity. The restoration of an active peptide conformation when A⁶ was removed to form NLPLRF-NH₂ supports the argument that increased mobility contributed to the functional results observed with hRFRP-1_(6–12).

G-protein-coupled receptors are associated with RF-NH₂ peptide signal transduction pathways.^{26–28} RFRP-1 binds to expressed GPCR proteins NPFF₁R and NPFF₂R.^{2,3,5,7} RFRP-1 and NPFF₂R are present in the brain, and NPFF₂R is known to exist in the heart;^{2–5,8,10,11} however, no previous report identified hRFRP-1 in the myocardium or the cellular location of NPFF₂R within the heart.^{2–5,8,10,11} In this study, transcripts for RFRP and NPFF₂R were detected in rat isolated cardiac myocytes and heart and human myocardium (Table 3, Figure 4). Although the investigated NPFF₁R transcript was not amplified from rat cardiomyocyte mRNA, NPFF₁R was detected in brain. The RFRP and NPFF₂R(s) transcript expression data and ability of hRFRP-1 to influence contractility in isolated cardiac myocytes support the conclusion that hRFRP-1 acts through NPFF₂R. Further, the observation that hRFRP-3 fails to influence contractility in isolated cardiomyocytes is consistent with the signaling pathway being hRFRP-1 specific. Additionally, the inability of RF9 to antagonize hRFRP-1 effects suggests that a difference exists between the receptor protein present in cardiomyocytes and the central nucleus of amygdala.¹⁴ These data also argue that a difference exists between the expressed receptor proteins and cardiomyocyte NPFF₂R to explain the selectivity of hRFRP-1 versus hRFRP-3 and RF9.

The unexpected maintenance of the Ca²⁺ transient when hRFRP-1 impaired contractile shortening indicated that the myofilament is a primary downstream target for this peptide (Figure 5A). The ability of Bis-1 to block the Ca²⁺ transient to hRFRP-1 independently supported our previous work showing that PKC inhibition attenuated the influence of hRFRP-1 on isolated cardiac myocytes (Figure 5B).⁹ This conclusion was further supported by the enhanced myofilament protein phosphorylation detected after hRFRP-1 treatment compared to controls and the absence of a phosphorylation response in myocytes treated with the receptor antagonist LPLAF-NH₂ (Figure 5C). In future studies, it will be important to address whether hRFRP-1 and/or its receptor is associated with pleiotropic activation via G-dependent and G-independent mechanisms found with other peptides such as angiotensin II.²⁹

In summary, SAR, transcript, Ca²⁺ transient, kinase inhibitor, and phospholabeling data presented here provided a roadmap to identify a first generation receptor antagonist of hRFRP-1 activity on cardiac performance and gain insight into a novel signaling pathway, which may be used for drug development.

These results provide strong evidence that a hRFRP-1 signaling pathway modulates contractile function in mammalian myocardium.

■ EXPERIMENTAL SECTION

Peptides. hRFRP-1, hRFRP-3, and analogues were synthesized on a 433A Applied Biosystems peptide synthesizer using standard Fmoc procedures and purified by reversed-phase high performance liquid chromatography. Each synthesis purity was obtained with $\geq 95\%$ and identified by matrix-assisted laser desorption/ionization time-of-flight mass spectrometry. Peptide nomenclature follows convention (Table 1); RFRP-1 represents RFamide-related peptide-1, [A[#]]hRFRP-1 represents an alanyl-substituted analogue of the full-length human parent peptide, RFRP-1, where the position of the alanine substitution is indicated by #. Truncated analogues are represented by hRFRP-1(#-#), where #-# represents the length of the peptide sequence, N terminus to C terminus; the numbers represent the amino acid positions.

Sarcomere Length Shortening. Adult rat ventricular cardiac myocytes were isolated as previously described.^{9,30} Hearts from Sprague–Dawley rats were perfused and enzymatically digested to isolate myocytes, which were plated on laminin-coated coverslips in serum-containing media for 2 h and then placed in serum-free media. Sarcomere shortening was measured in a 37 °C cell chamber with myocytes paced at 0.2 Hz using a video-based detection system (IonOptix; see www.ionoptix.com for a detailed protocol on how to measure cardiomyocyte contractility) as previously described.^{9,30} Signal averaged data were analyzed to determine resting sarcomere length, peak shortening amplitude (peak shortening), shortening rate (departure velocity), and relengthening rate (return velocity) under basal conditions and then in response to 20 min of treatment with 10 nM peptide or analogue or media alone (e.g., control) in 7–20 myocytes from three to four rat hearts by two different investigators, one of which did recordings blind, without knowledge of the reagent applied. Values reported are expressed as the mean \pm standard error of mean (SEM) for the percent change relative to baseline. Values reported in Table 1 are percent hRFRP-1 activity based on mean values where hRFRP-1 activity is defined as 100%. Errors in Table 1 were calculated following the protocol for propagation of error. Data were analyzed using an unpaired two-tailed *t* test with a 95% confidence interval (GraphPad Prism); statistical significance compared to hRFRP-1 was established at $p \leq 0.05$.

Echocardiography. Echocardiograms were collected as previously described⁹ according to the recommendations of the American Society of Echocardiography by a single, registered echocardiographer. Female C57BL/6 mice were weighed to calculate the amount of peptide delivered per kilogram body weight (kg bw). Saline, analogue, peptide, or analogue and peptide ($n = 4-5$) were delivered intravenously via tail-vein injection in a maximum volume of 50 μ L to achieve an initial delivery of 250 nmol of hRFRP-1/kg bw. Recordings were taken prior to delivery of the injectant and used as a baseline for the individual animal. Each animal was used only once for one injectant. All animal protocols were approved by the University of Michigan (UM) Committee on Use and Care of Animals (UCUCA).

Polymerase Chain Reaction. Extraction of RNA from isolated rat cardiac myocytes, heart, and brain and human heart was performed using TRIzol (Invitrogen). All animal protocols were approved by the UM UCUCA. Whole rat hearts and brains were removed under anesthesia, after which the animal was humanely euthanized; tissue was stored at -80 °C until RNA extraction. Failing human heart was perfused to cardioplegia prior to explant in preparation for donor heart implantation. This protocol was approved by the Institutional Review Board of the UM Medical School. Tissue samples were deidentified from information about age, sex, and diagnosis. Pieces of tissue, from the discarded heart, were immediately frozen in liquid N₂ and stored at -80 °C until RNA extraction.

First strand cDNA was synthesized at 37 °C using random hexamers (Invitrogen) and M-MuLV reverse transcriptase (New England Bio Labs). All primer sequences were verified using the NCBI

Primer BLAST primer design tool and purchased from Invitrogen. Polymerase chain reactions were done at melting temperatures appropriate for primer sequences and extended at 72 °C from 30 s to 1 min depending on product length; cycle numbers were optimized for product production. Ethidium bromide stained DNA bands were cut from agarose gels, eluted using a QIAquick gel extraction kit (Qiagen), and subjected to automated Sanger sequencing. Controls included no reverse transcriptase, no primers, 26RFa, GRP103, and ET-1.¹⁵⁻¹⁷

Quantitative Polymerase Chain Reaction. Extraction of RNA from rat cardiac myocytes, heart, and brain was performed using TRIzol (Invitrogen). All RNA samples were DNase (Ambion) treated prior to qPCR and transcribed using random hexamers and GoScript reverse transcriptase (Promega). Amplification of qPCR products was measured using GoTaq qPCR master mix (Promega) with a Bio-Rad CFX 96 C1000 real-time PCR instrument. After 50 cycles, reactions were analyzed with a thermal melting curve. All C_T values were determined with Bio-Rad CFX Manager software. Relative differences in expression were calculated using the comparative C_T method.^{19,20} $\Delta C_T = C_{Ttarget} - C_{Treference}$ was calculated to normalize the average C_T value for each target to the average C_T of Rpl32, the reference transcript.¹⁸ The $\Delta\Delta C_T$ was then calculated for targets: $\Delta\Delta C_T = \Delta C_{Ttarget\ tissue} - \Delta C_{Treference\ tissue}$. *N*-Fold expression of the target transcripts relative to brain tissue was calculated using a ratio of $2^{-\Delta\Delta C_T}$. Controls included no reverse transcriptase, no primers, and 26RFa.^{15,16}

Ca²⁺ Transient. Simultaneous measurements of the Ca²⁺ transient and myocyte shortening were made in a separate group of isolated cells loaded with Fura-2AM, as described earlier.³¹ Signal averaged measurements of resting and peak Fura-2AM ratios, the rate of Ca²⁺ rise and decay, time to 25%, 50%, and 75% decay (TTD_{25%}, TTD_{50%}, and TTD_{75%}), and sarcomere shortening were made at 0.2 Hz (37 °C) in rat myocytes under basal conditions and in response to 20 min of treatment with hRFRP-1 (10 nM) with and without protein kinase inhibitors, which included the PKC inhibitor Bis-1 (500 nM) and the PKA inhibitor PKI (200 nM). Results for control, physiological saline ($n = 3$), and hRFRP-1-treated ($n = 8$) rat myocytes were compared using an unpaired Student's *t* test with $p \leq 0.05$ considered statistically significant.

Protein Phosphodetection. Phosphorylation of downstream targets was studied in radiolabeled myocytes, as described earlier.²³ Myocytes labeled with ³²P-orthophosphate (100 μ Ci) for 2 h at 37 °C were transferred to unlabeled M199 media containing 10 nM calyculin A (basal) or the same media with 10 nM hRFRP-1 or LPLAF-NH₂ for 10 min at 37 °C. Phosphorylation was terminated in ice-cold relaxing solution (RS; 7 mM EGTA, 20 mM imidazole, 1 mM free Mg²⁺, 14.5 mM creatine phosphate, and 4 mM MgATP with KCl added to yield an ionic strength of 180 mM, pH 7) containing 0.5% TX-100 to permeabilize myocytes. The myocytes were immediately collected in ice-cold sample buffer. Each sample was vortexed, boiled for 1 min, and placed on ice until loaded on a 12% SDS–PAGE gel for protein separation. Gels were silver stained and dried, and phosphorylation was determined after an overnight exposure in a phosphor-image cassette.

■ ASSOCIATED CONTENT

Supporting Information

Tables containing sequences, T_m , and product lengths for PCR and qPCR primers and figures including RFRP-1 consensus and PCR product sequence data. This material is available free of charge via the Internet at <http://pubs.acs.org>.

■ AUTHOR INFORMATION

Corresponding Author

*Phone: 734-764-4467. Fax: 734-763-4581. E-mail: nicholsr@umich.edu.

Author Contributions

[∞]The second, third, and fourth authors are listed alphabetically by surname.

Notes

The authors declare no competing financial interest.

ACKNOWLEDGMENTS

This work was supported by a NIH Grant R21HL093627 to R.N., a Concept to Commercialization Funding from the University of Michigan Medical Innovation Center and a University of Michigan Cardiovascular Center Innovative Grant to R.N., and Grant R01HL067254 to M.V.W.

ABBREVIATIONS USED

GPCR, G-protein-coupled receptor; FaRP, FMRF-NH₂-related peptide; hRFRP-1, human RFamide-related peptide-1; hRFRP-3, human RFamide-related peptide-3; NPFF₁R, NPFF receptor 1; NPFF₂R, NPFF receptor 2; SAR, structure–activity relationship; PKC, protein kinase C; SEM, standard error of the mean; kg bw, kilogram body weight; EF, ejection fraction; FS, fractional shortening; UM, University of Michigan; UCUCA, University Committee on Use and Care of Animals; ET-1, endothelin-1; C_T, threshold cycle; 26RFa, 26RFamide; TTD, time to decay; Bis-1, bis-indolylmaleimide

REFERENCES

- (1) Price, D. A.; Greenberg, M. J. Structure of a molluscan cardioexcitatory neuropeptide. *Science* **1977**, *197*, 670–671.
- (2) Hinuma, S.; Shintani, Y.; Fukusumi, S.; Iijima, N.; Matsumoto, Y.; Hosoya, M.; Fujii, R.; Watanabe, T.; Kikuchi, K.; Terao, Y.; Yano, T.; Yamamoto, T.; Kawamata, Y.; Habata, Y.; Asada, M.; Kitada, C.; Kurokawa, T.; Onda, H.; Nishimura, O.; Tanaka, M.; Ibata, Y.; Fujino, M. New neuropeptides containing carboxy-terminal RFamide and their receptor in mammals. *Nat. Cell Biol.* **2000**, *2*, 703–708.
- (3) Liu, Q.; Guan, X. M.; Martin, W. J.; McDonald, T. P.; Clements, M. K.; Jiang, Q.; Zeng, Z.; Jacobson, M.; Williams, D. L.; Jr, Yu, H.; Bomford, D.; Figueroa, D.; Mallee, J.; Wang, R.; Evans, J.; Gould, R.; Austin, C. P. Identification and characterization of novel mammalian neuropeptide FF-like peptides that attenuate morphine-induced antinociception. *J. Biol. Chem.* **2001**, *276*, 36961–36969.
- (4) Ubuka, T.; Morgan, K.; Pawson, A. J.; Osugi, T.; Chowdhury, V. S.; Minakata, H.; Tsutsui, K.; Millar, R. P.; Bentley, G. E. Identification of human GnIH homologs, RFRP-1 and RFRP-3, and the cognate receptor, GPR147 in the human hypothalamic pituitary axis. *PLoS One* **2003**, *4*, e8400.
- (5) Fukusumi, S.; Habata, Y.; Yoshida, H.; Iijima, N.; Kawamata, Y.; Hosoya, M.; Fujii, R.; Hinuma, S.; Kitada, C.; Shintani, Y.; Suenaga, M.; Onda, H.; Nishimura, O.; Tanaka, M.; Ibata, Y.; Fujino, M. Characteristics and distribution of endogenous RFamide-related peptide-1. *Biochim. Biophys. Acta* **2001**, *1540*, 221–232.
- (6) Nichols, R. Isolation and structural characterization of *Drosophila* TDVDHVFLRFamide and FMRFamide-containing neural peptides. *J. Mol. Neurosci.* **1992**, *3*, 213–218.
- (7) Fukusumi, S.; Habata, Y.; Yoshida, H.; Iijima, N.; Kawamata, Y.; Hosoya, M.; Fujii, R.; Hinuma, S.; Kitada, C.; Shintani, Y.; Suenaga, M.; Onda, H.; Nishimura, O.; Tanaka, M.; Ibata, Y.; Fujino, M. Recent advances in mammalian RFamide peptides: the discovery and functional analyses of PrRP, RFRPs and QRFP. *Peptides* **2006**, *27*, 1073–1086.
- (8) Yano, T.; Iijima, N.; Kakahara, K.; Hinuma, S.; Tanaka, M.; Ibata, Y. Localization and neuronal response of RFamide related peptides in the rat central nervous system. *Brain Res.* **2003**, *982*, 156–167.
- (9) Nichols, R.; Demers, L. A.; Larsen, B. M.; Robinson, D.; Converso, K.; Russell, M. W.; Westfall, M. V. Human RFamide-related peptide-1 diminishes cellular and integrated cardiac contractile performance. *Peptides* **2010**, *31*, 2067–2074.

- (10) Bonini, J. A.; Jones, K. A.; Adham, N.; Forray, C.; Artymyshyn, R.; Durkin, M. M.; Smith, K. E.; Tamm, J. A.; Boteju, L. W.; Lakhani, P. P.; Raddatz, R.; Yao, W. J.; Ogozalek, K. L.; Boyle, N.; Kouranova, E. V.; Quan, Y.; Vaysse, P. J.; Wetzel, J. M.; Branchek, T. A.; Gerald, C.; Borowsky, B. Identification and characterization of two G protein-coupled receptors for neuropeptide FF. *J. Biol. Chem.* **2000**, *275*, 39324–39331.

- (11) Elshourbagy, N. A.; Ames, R. S.; Fitzgerald, L. R.; Foley, J. J.; Chambers, J. K.; Szekeres, P. G.; Evans, N. A.; Schmidt, D. B.; Buckley, P. T.; Dytko, G. M.; Murdock, P. R.; Milligan, G.; Groarke, D. A.; Tan, K. B.; Shabon, U.; Nuthulaganti, P.; Wang, D. Y.; Wilson, S.; Bergsma, D. J.; Sarau, H. M. Receptor for the pain modulatory neuropeptides FF and AF is an orphan G protein-coupled receptor. *J. Biol. Chem.* **2000**, *275*, 25965–25971.

- (12) Eipper, B. A.; Stoffers, D. A.; Mains, R. E. The biosynthesis of neuropeptides: peptide alpha-amidation. *Annu. Rev. Neurosci.* **1992**, *15*, 57–85.

- (13) Simonin, F.; Schmitt, M.; Laulin, J. P.; Laboureyras, E.; Jhamandas, J. H.; MacTavish, D.; Matifas, A.; Mollereau, C.; Laurent, P.; Parmentier, M.; Kieffer, B. L.; Bourguignon, J. J.; Simonnet, G. RF9, a potent and selective neuropeptide FF receptor antagonist, prevents opioid-induced tolerance associated with hyperalgesia. *Proc. Natl. Acad. Sci. U.S.A.* **2006**, *103*, 466–471.

- (14) Kovács, A.; László, K.; Gálósi, R.; Tóth, K.; Ollmann, T.; Péczely, L.; Lénárd, L. Microinjection of RFRP-1 in the central nucleus of amygdala decreases food intake in the rat. *Brain Res. Bull.* **2012**, *88*, 589–595.

- (15) Fukusumi, S.; Yoshida, H.; Fujii, R.; Maruyama, M.; Komatsu, H.; Habata, Y.; Shintani, Y.; Hinuma, S.; Fujino, M. A new peptidic ligand and its receptor regulating adrenal function in rats. *J. Biol. Chem.* **2003**, *278*, 46387–46395.

- (16) Jiang, Y.; Gustafson, E. L.; Yadav, D.; Laverty, M.; Murgolo, N.; Vassileva, G.; Zeng, M.; Laz, T. M.; Behan, J.; Qiu, P.; Wang, L.; Wang, S.; Bayne, M.; Greene, J.; Monsma, F., Jr.; Zhang, F. L. Identification and characterization of a novel RF-amide peptide ligand for orphan G-protein-coupled receptor SP9155. *J. Biol. Chem.* **2003**, *278*, 27652–27657.

- (17) Suzuki, T.; Kumazaki, T.; Mitsui, Y. Endothelin-1 is produced and secreted by neonatal rat cardiac myocytes in vitro. *Biochem. Biophys. Res. Commun.* **1993**, *191*, 823–830.

- (18) Brattellid, T.; Winer, L. H.; Levy, F. O.; Liestøl, K.; Sejersted, O. M.; Andersson, K. B. Reference gene alternatives to *Gapdh* in rodent and human heart failure gene expression studies. *BMC Mol. Biol.* **2010**, *11*, 22–31.

- (19) Livak, K. J.; Schmittgen, T. D. Analysis of relative gene expression data using real-time quantitative PCR and the 2⁻(Delta Delta C(T)) method. *Methods* **2001**, *25*, 402–408.

- (20) Schmittgen, T. D.; Livak, K. J. Analyzing real-time PCR data by the comparative C(T) method. *Nat. Protoc.* **2008**, *3*, 1101–1108.

- (21) Westfall, M. V.; Turner, I.; Albayya, F. P.; Metzger, J. M. Troponin I chimera analysis of the cardiac myofilament tension response to protein kinase A. *Am. J. Physiol.: Cell Physiol.* **2001**, *280*, C324–C332.

- (22) Braz, J. C.; Gregory, K.; Pathak, A.; Zhao, W.; Sahin, B.; Kleivitsky, R.; Kimball, T. F.; Lorenz, J. N.; Nairn, A. C.; Liggett, S. B.; Bodi, I.; Wang, S.; Schwartz, A.; Lakatta, E. G.; DePaoli-Roach, A. A.; Robbins, J.; Hewett, T. E.; Bibb, J. A.; Westfall, M. V.; Kranias, E. G.; Molkentin, J. D. PKC-alpha regulates cardiac contractility and propensity toward heart failure. *Nat. Med.* **2004**, *10*, 248–254.

- (23) Westfall, M. V.; Borton, A. R. Role of troponin I phosphorylation in protein kinase C-mediated enhanced contractile performance of rat myocytes. *J. Biol. Chem.* **2003**, *278*, 33694–33700.

- (24) Miniño, A. M.; Murphy, S. L.; Xu, J.; Kochanek, K. D. Deaths: Final Data for 2008. *National Vital Statistics Reports*; National Center for Health Statistics: Hyattsville, MD, 2011; Vol. 59, No. 10.

- (25) Le Marec, O.; Neveu, C.; Lefranc, B.; Dubessy, C.; Boutin, J. A.; Do-Régo, J. C.; Costentin, J.; Tonon, M. C.; Tena-Sempere, M.; Vaudry, H.; Leprince, J. Structure–activity relationships of a series of

analogues of the RFamide-related peptide 26RFa. *J. Med. Chem.* **2011**, *54*, 4806–4814.

(26) Meeusen, T.; Mertens, I.; Clynen, E.; Baggerman, G.; Nichols, R.; Nachman, R. J.; Huybrechts, R.; De Loof, A.; Schoofs, L. Identification in *Drosophila melanogaster* of the invertebrate G protein-coupled FMRFamide receptor. *Proc. Natl. Acad. Sci. U.S.A.* **2002**, *99*, 15363–15368.

(27) Egerod, K.; Reynisson, E.; Hauser, F.; Cazzamali, G.; Williamson, M.; Grimmelikhuijzen, C. J. Molecular cloning and functional expression of the first two specific insect myosuppressin receptors. *Proc. Natl. Acad. Sci. U.S.A.* **2003**, *100*, 9808–9813.

(28) Kubiak, T. M.; Larsen, M. J.; Burton, K. J.; Bannow, C. A.; Martin, R. A.; Zantello, M. R.; Lowery, D. E. Cloning and functional expression of the first *Drosophila melanogaster* sulfakinin receptor DSK-R1. *Biochem. Biophys. Res. Commun.* **2002**, *291*, 313–320.

(29) Hunyady, L.; Catt, K. J. Pleiotropic AT1 receptor signaling pathways mediating physiological and pathogenic actions of angiotensin II. *Mol. Endocrinol.* **2005**, *20*, 953–970.

(30) Westfall, M. V.; Rust, E. M.; Albayya, F.; Metzger, J. M. Adenovirus-mediated myofibrillar gene transfer into adult cardiac myocytes. *Methods Cell Biol.* **1997**, *52*, 307–322.

(31) Westfall, M. V.; Lee, A. M.; Robinson, D. A. Differential contribution of troponin I phosphorylation sites to the endothelin-mediated contractile response. *J. Biol. Chem.* **2005**, *280*, 41324–41331.